6th Micro and Nano Flows Conference
Atlanta,USA, 9-12 September 2018

Particle and Red Blood Cell Concentration Distributions in Narrow Microchannel Flows with Wall Effects

Kazuya TATSUMI*, Shinnosuke NOGUCHI, Akira TATSUMI, Reiko KURIYAMA, Kazuyoshi NAKABE

* Corresponding author: Tel.: +81-75-383-3606; Fax: +81-75-383-3608; Email: tatsumi@me.kyoto-u.ac.jp
Department of Mechanical Engineering and Science, Kyoto University Kyoto, Japan

Keywords: Microchannel Flows, Red Blood Cells, Particles, Collision model, Wall Effects, Number Density

1. Introduction

Diffusion and motions of particle and blood cell in blood flow and particle-concentrated flows are essential phenomena in the fields of medicine, biology and microfluidic systems in terms of understanding the mass and momentum transfer rates at blood vessels walls, and developing drug delivery systems and lab-on-a-chip devices. The concentration distribution and mass flux of the solute and other objects are influenced by the motion and number density distribution (concentration) of the particle and blood cell in the flow. Therefore, many studies have been made in this field [1]. However, particles and blood cell concentration distributions and mass transfer for highly concentrated flows in channels with characteristic length of several cell, in which the wall effects are significant, is not known well. In this study, we measured the particle and red blood cell concentration in microchannel flow and applied analytical models considering the particle-particle collision, fluid dynamic force and wall effects.

2. Experimental Methods and Conditions

Figure 1 (a) shows the schematic of the microchannel. Particles and RBCs mixed fluids were supplied to the straight channel inlet by the pressure controlled-type flow pump. The straight channel region split into three channels by two partitions with edge shaped leading ends. This configuration produced a uniform number density distribution at the inlet of the center channel in which the measurement was conducted. The width and height of this area were 28μm and 27μm, respectively. Images of the particles and RBCs were measured by a microscope and high-speed video camera. The images were analyzed by ImageJ to obtain the number density distributions. Figs. 1 (b) and (c) show the examples of the images.

Micro polystyrene particles 5μm and 8μm in diameters (Microparticles GmbH, PS-R-5.0, PS-R-8.1) were used for particles. Red blood cells were collected from healthy volunteers. We rigidized the RBCs by suspending the collected concentrated RBCs in 0.025% glutaraldehyde mixed phosphate buffered saline solution. We removed the effects of tank treading motions of the red blood cells in order to focus on the effects of rotational motions, and collisions between the cells and wall.

The microchannel and particles were washed by 10wt% bovine serum albumin (BSA: Sigma-Aldrich, A2153-50G) water solution to coat the surface and prevent the adhesion and aggregation. The particles and RBC were respectively mixed with 10wt% BSA solution and 0.1wt% sodium lauryl sulfate (Nacalai tesque) solution. Hematocrit (Hct) of the particle and RBC solutions were varied in the range of 9.2~16.6%. The flow rate was 0.6μL/min. Reynolds number based on the channel height and particle diameter (8μm) in this cases were 0.23 and 5.9×10^{-4}, respectively.

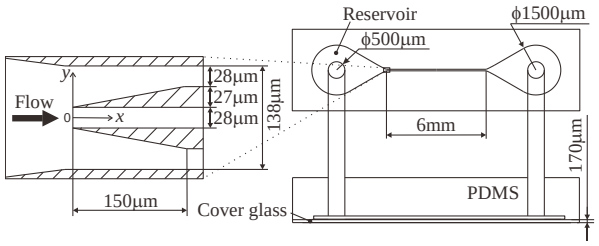

(a) Microchannel and measurement area

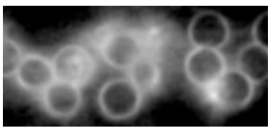

(b) Images of particles

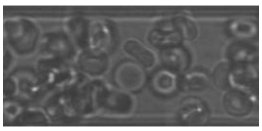

(c) Images of RBC

Figure 1. *Schematic of the microchannel and recorded images of 8□m particles and red blood cells (the flow is from the left to the right).*

3. Results and Discussion

3.1 Particle concentration distribution

Figure 2 shows the number density (concentration) ϕ distributions in the channel spanwise direction for 5μm and 8μm particles. The distributions show the results obtained at the streamwise locations of x=0, 3,000 and 6,000μm. $\overline{\phi}$ is the spanwise average value of ϕ. In the case of Hct=11.7% for 8μm particles shown in Fig. 2 (a), a uniform profile is observed in the channel center region (y/w~0) at x=0μm. $\phi/\overline{\phi}$ in this region increases in the downstream and converges to a distribution showing maximum peaks at the channel center and channel walls. This trend is also observed in Fig. 2 (b) for the case of Hct=16.6%. In the case of 5μm diameter particles, similar distribution and characteristics are also obtained while a third peak additionally appears in the middle of the two peaks at y/w~0.25.

To understand the factors producing these distributions, one-dimensional computation solving the particle concentration conservation equation shown in Eq. (1) and employing the model considering the particle-particle collision, fluid dynamic force and wall effects was conducted. The first term in Eq. (1) is the convection term for the streamwise direction. v_c and v_f in the second term are the velocity (flux) attributed to the particle-particle collisions [1, 2] and fluid dynamic force exerted on the particles.

$$u_p \frac{\partial \phi}{\partial x} + \frac{\partial}{\partial y}\left((v_c + v_f)\phi\right) = 0 \quad (1)$$

v_c is based on the collision rate and displacement of the particle once the collision occurs and is obtained by Eq. (2).

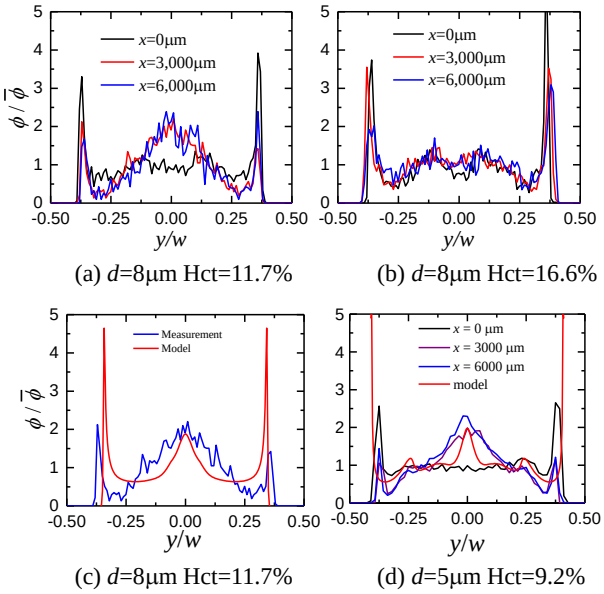

(a) d=8μm Hct=11.7% (b) d=8μm Hct=16.6%

(c) d=8μm Hct=11.7% (d) d=5μm Hct=9.2%

Figure 2. *Particle number density (concentration) distributions in the channel spanwise direction.*

$$v_c(y) = K\int_{-d}^{d} l(y,s)\cdot\phi(y+s)\cdot|u(y+s)-u(y)|\cdot 2\sqrt{d^2-s^2}\,ds \quad (2)$$

l is the displacement of particles when colliding with neighboring particles. y is the spanwise location of the particle of interest and s is the distance from the center of this particle. The collision rate is proportional to ϕ and the velocity difference with the colliding particles.

Lift force exerted on the particle was referred to the analytical results [3] and was applied to the Stokes equation to derive the resulting particle velocity v_l. Further, we considered the wall effect by considering the distance between the particle and wall in the integration region of Eq. (2) and displacement l.

Fig. 2 (c) shows the computational results. The model correctly presents the maximum peaks at the channel center and near wall regions. Furthermore, the distribution agrees reasonably well with the measurement. The increase of ϕ observed at the channel center was attributed to the parabolic velocity profile of the Poiseuille flow in which the shear rate decreases toward the channel center. On the other hand, the modification of the asymmetric distribution of the collision rate on both sides of the particles due to the wall effect produces the peaks at the wall.

In the case of 5μm diameter particle, the model presents the third peak at the same position with reasonable accuracy. This third peak was attributed to the high concentration of particles flowing along the channel wall. As the particles are packed at the wall surface, the second layer of particles is formed with distance of one particle diameter from the wall.

3.2 Red blood cell concentration distribution

Concentration ϕ distribution of the RBCs is shown in Fig. 3 for the half-side of the channel. Compared to the 8μm diameter particle distribution, the maximum peak observed at the channel sidewall decreases and a third peak appears at the location of approximately y/w=0.3. The rotating motion of the RBC is believed to be the main factor for these characteristics. The "tumbling" motion of RBC increases the collision rate between the RBCs and with the wall compared with the RBC in steady state. Larger displacement and spanwise velocity for the RBC is produced in this case especially in the near wall region.

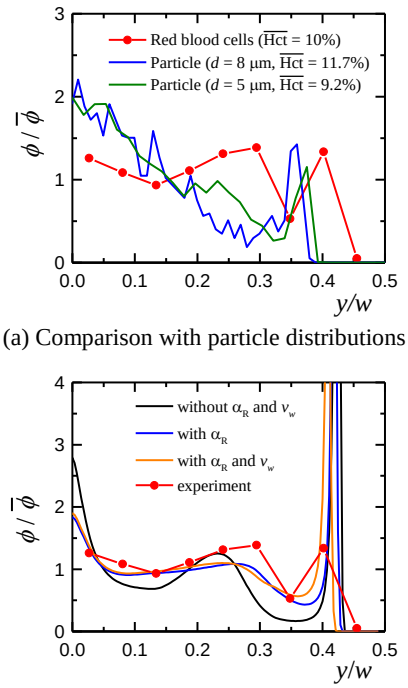

(a) Comparison with particle distributions

(b) Comparison with model

Figure 3. *RBC number density distributions in the spanwise direction (Hct=10%).*

We applied this effect to the model by modifying the collision rate and adding another spanwise velocity (flux) v_R to the second term of Eq. (1). Collision rate was modified by a weighting factor α_R which was based on the distance s. v_R was defined as $v_R = K_R l_R \dot{\gamma}$ where l_R and $\dot{\gamma}$ are the displacement due to collision in the RBC case and the flow shear rate, respectively.

The computational result is shown in Fig. 3 (b). The third peak is produced by the model and the distribution matches well with the measurement particularly when α_R and v_w are both applied to the model. The peak observed in the near wall region slightly decreases compared with the particle case. Further modification, threrefore, is still required for the parameters in the model to produce larger wall effects. Nevertheless, we can obtain the fundamental characteristics of the ϕ distribution and may derive the conclusion that the smaller effective length of the RBC and the collision of the RBC with the wall due to the RBC rotation decreases the concentration at wall and produces a third peak in the concentration distribution.

4. Conclusions

We measured and calculated the particle and RBC concentration distributions for flow in channel with narrow width and showed that the particle size, Hct, and the shape and motion of the RBC affect the distributions. The wall effect was significant and the wall function model we showed agreed reasonably well with the measurement. Further study on varying the conditions, considering the deformation and tank treading motion of the RBC, and applying the volumetric concentration to the model is required as future work.

References

[1] X. Grandchamp et al., *Physical Review Letters*, (2013) Vol. 110, 108101.
[2] D. Leighton and A. Acrivos, *J. Fluid Mech*, (1987) Vol. 181, pp. 415-439.
[3] R. J. Phillips, R. C. Armstrong, R. A. Brown, A. L. Graham and J. R. Abbott, *Physics of Fluids*, (1991) Vol. 4, pp. 30-40.
[4] B. P. Ho and L. G. Leal, *J. Fluid Mech*, (1974) Vol. 65, pp. 365-400.